Dynamical scaling analysis on critical universality class for fully frustrated XY models in two dimensions

Yukiyasu Ozeki ⬤, Yuri Yajima, and Yuka Nakamura

Department of Engineering Science, Graduate School of Informatics and Engineering, The University of Electro-Communications,
1-5-1 Chofugaoka, Chofu-shi, Tokyo 182-8585, Japan

Critical properties of the fully frustrated XY models on square and triangular lattices are investigated by means of the nonequilibrium relaxation (NER) method. We examine the validity of the conclusion on the universality class of the chiral transition previously obtained by the NER method, in which that belongs to a non-Ising-type one. To clarify it, we analyze the NER of fluctuations for longer Monte Carlo steps on lager lattices than those performed previously. The calculation is made at the chiral transition temperatures estimated carefully by the use of recently improved dynamical scaling analysis. The result indicates that the asymptotic behavior of the time-dependent exponents, which should converge to the critical exponents, show the same tendency as those obtained previously in shorter times. We also apply the improved dynamical scaling analysis to the estimation of Kosterlitz-Thouless (KT) transitions and confirm the existence of the double transitions for the chiral and KT phases with more reliable estimations.

I. INTRODUCTION

The frustrated magnetic systems have been studied extensively [1–4] in statistical physics because of their rich phase diagrams, the possibility of new universality classes, and the slow dynamics in the relaxation. The triangular antiferromagnetic (AF) XY model is a typical example [4–12]. Together with the frustrated model on the square lattice [3,6–8,10,12–25], they are called the fully frustrated (FF)XY models in two dimensions, which have attracted much attention in recent decades.

In FFXY models in two dimensions, the possibility of two different transitions, the chiral transition and the Kosterlitz-Thouless (KT) one, has been discussed. Since the pioneering works [3,4] presented in the literature, there has been a controversy concerning the transition temperatures T_c and T_{KT} for these transitions: the double transitions ($T_c > T_{KT}$) or the single transition ($T_c = T_{KT}$). Another controversy has arisen concerning the universality class for the chiral transition [5]. The broken symmetry for the chiral transition is a discrete Z_2 one, which is the same as the Ising model. It is natural to expect the Ising class ($\nu = 1, \beta = 1/8, \dots$); however, some numerical studies indicated different ones [10,11,16,18,19]. Olsson [21,22] claimed that similar results indicating a non-Ising class obtained by the equilibrium Monte Carlo simulation (EMCS) with finite-size scaling analysis were an artifact due to the smallness of simulations. Many works have been devoted to these problems, although they have remained unsolved because of the frustration.

The EMCS has been widely used for phase transitions and critical phenomena. Although it works even in frustrated systems, it sometimes suffers difficulties in the analysis due to slow relaxation in low-temperature regime, which restricts the available system sizes to ones that are too small. The nonequilibrium relaxation (NER) method is an efficient numerical technique for analyzing equilibrium phase transitions [26]. One may observe the relaxation of the order parameter (e.g., the magnetization in the ferromagnet) in the thermalization process from the complete ordered state. It provides the critical temperature and critical exponents accurately.

In Ref. [27], one of the authors investigated these problems by means of the NER method. The chiral transition temperature and the KT one were estimated precisely, where these two transitions occur at different temperatures ($T_c > T_{KT}$) for both square- and triangular-lattice systems. This confirms the double transitions and the existence of the intermediate phase. Using the NER of fluctuations, the critical exponents of the chiral transition were also estimated, which indicates that the chiral transition belongs to the same universality class for both models, but it is different from the Ising class in two dimensions. These conclusions of the NER method were almost consistent with the tendency of other works in those days [10,11,16,18,19]. In opposition to Olsson's claim [21,22], we have argued the validity of our picture, which was confirmed by the estimated exponents being identical asymptotically for both lattice systems.

After that, Obuchi and Kawamura [28] performed EMCS with large-scale and careful scaling analysis. In their results, the double transition was observed consistently with the NER result. On the universality class of the chiral transition, while the values of estimated exponents deviated from those in the Ising class, Obuchi and Kawamura argued that the deviation came from the finite-size effect, and these exponents should approach the Ising values in the thermodynamic limit, i.e., an argument similar to Olsson's claim. They also criticized the NER result [26,27], saying it may include a short-time effect and should approach the Ising values in a longer-time observation.

Recently, the dynamical scaling analysis of the NER data has been improved by using the Bayesian inference and the kernel method [29,30]. Together with the pinching estimation used formerly, the transition points can be estimated efficiently and precisely with a reliable error bar. In the present study, we apply the NER method to both triangular- and square-lattice systems. Performing simulations on lager lattices in a longer-time interval at a carefully estimated transition temperature, we deny the criticism of the finite-time effect in the previous work. Comparing the results of the two models would be helpful in seeing the validity and efficiency of analyses. Using the accurate transition temperature from the improved analysis, we can estimate reliable critical exponents and confirm the non-Ising-type universality class for the chiral transition and the possibility of the double transition.

The remainder of this paper is organized as follows. The models are explained in Sec. II. The order parameters are also defined. In Sec. III, the estimation process of the transition temperature from NER data is explained for both the old analysis and the improved one. The chiral transition temperature is estimated for both FFXY models by using the improved analysis in Sec. IV. In Sec. V, the critical exponents for the chiral transition are estimated using the NER of fluctuations, and the universality class is discussed. The KT transition temperature is estimated in Sec. VI using the improved dynamical scaling analysis. Section VII gives a summary of this study and our results.

II. MODELS

We study FFXY models on both square and triangular lattices. The Hamiltonian is expressed as

$$\mathcal{H} = -J \sum_{\langle ij \rangle} \omega_{ij} \cos(\theta_i - \theta_j), \qquad (2.1)$$

where $0 \leqslant \theta_i < 2\pi$ and $J > 0$. The summation $\langle ij \rangle$ is taken over all nearest-neighbor sites on the lattices. The constant ω_{ij} takes -1 for all bonds on the triangular-lattice system, which represents nothing but an AF interaction. It takes $+1$ for three of four bonds on a plaquette and -1 for the other one on the square-lattice system. These lattices are shown in Fig. 1.

Let us consider the ground state for these models. They have structures with clockwise or counterclockwise rotation on each plaquette in two subplaquette patterns (see Fig. 1). The system has Z_2 symmetry due to this clockwise-counterclockwise degeneracy and a continuous $U(1)$ symmetry due to the global rotation with respect to the spin orientation. For the triangular-lattice system, a three-sublattice structure appears with angular difference $2\pi/3$: $\theta_A = 0$, $\theta_B = 2\pi/3$, and $\theta_C = 4\pi/3$. For the square-lattice system, a four-sublattice structure appears with angular difference $\pi/4$: $\theta_A = 0$, $\theta_B = \pi/4$, $\theta_C = \pi/2$, and $\theta_D = 3\pi/4$.

The ordering with the breakdown of the Z_2 symmetry is called the chiral ordering, in which the order parameter is the z component of the vector chirality. The order parameter with respect to the $U(1)$ symmetry is a magnetization modulated with θ_X for the X sublattice [$X = A, B, C, (D)$]. In the standard NER analysis, the initial state of relaxation is chosen to be one of the ground states. Let us denote the initial values of relaxation as θ_i^0, which are θ_X defined above. In the present
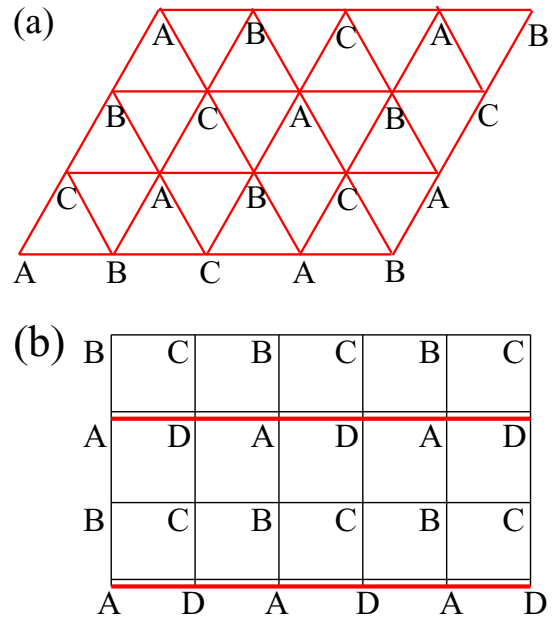

FIG. 1. Structure of lattices and initial states in the NER analysis (a) for the triangular-lattice system and (b) for the square-lattice one. They are one of the ground states with $\kappa = m_O = 1$ for each model. For the square lattice, the double line indicates the AF interactions, and the others indicate the ferromagnetic ones.

case, we calculate two kinds of order parameters at each time t: the chiral order parameter

$$\kappa(t) = \frac{a}{N} \sum_{(i \to j)} \langle \sin[\theta_i(t) - \theta_j(t)] \rangle, \qquad (2.2)$$

which is the z component of the vector chirality, and the spin orientational order parameter

$$m_O(t) = \frac{1}{N} \sum_i \langle \cos[\theta_i(t) - \theta_i^0] \rangle, \qquad (2.3)$$

which represents the projection of the spin component onto the direction of the initial state and detects the ordering with respect to the $U(1)$ symmetry. N is the number of spins, and a is a normalization factor as $a = 2/3\sqrt{3}$ or $a = 1/2\sqrt{2}$. The angular brackets $\langle \cdots \rangle$ represent a dynamical average, which can be evaluated by averaging over independent samples of relaxation from the identical initial state. The summation of $(i \to j)$ is taken for all bonds with a fixed order, $(A \to B \to C \to A)$ for the triangular lattice and $(A \to B \to C \to D, A \to D)$ for the square lattice; note that the sign of the $A \to D$ bond is opposite to the others. The initial states in Fig. 1 give $\kappa(0) = m_O(0) = 1$.

III. ESTIMATION OF THE TRANSITION TEMPERATURE USING THE NER METHOD

To estimate critical exponents using the NER method, one needs to calculate the NER of fluctuations just at the transition temperature. In the standard NER analysis [26] for second-order transitions, the so-called "pinching" method has been applied to estimate a reliable transition temperature, which was used for the estimation in the previous work [27]. Recently, we developed an improved dynamical scaling
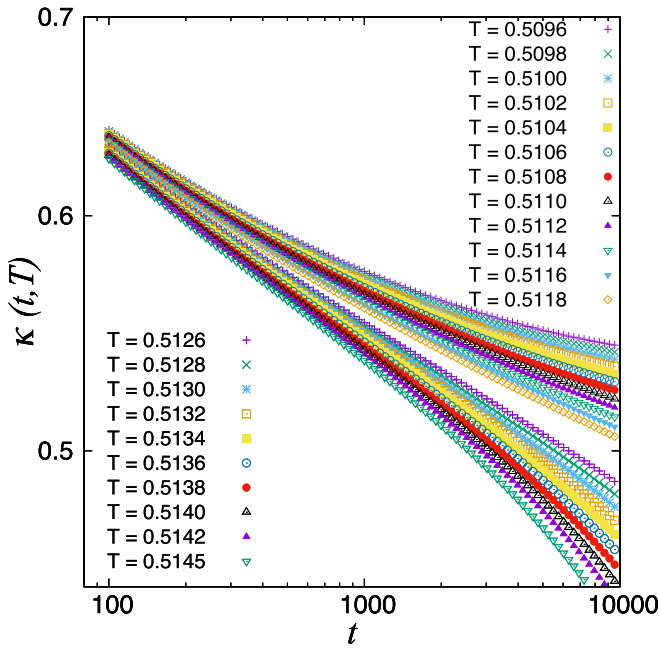
FIG. 2. Relaxation of the chiral order parameter $\kappa(t, T)$ for the triangular-lattice system in $0.5096 \leqslant T \leqslant 0.5118$ and in $0.5126 \leqslant T \leqslant 0.5145$ plotted on a double-logarithmic scale.

analysis scheme for the estimation of the precise transition temperature for both KT and second-order transitions [29,30]. Thus, we first update the estimation of the chiral transition temperature using both the pinching method and the improved dynamical scaling. The method for the KT transition will be discussed in Sec. VI.

Let us explain the pinching method. The NER analysis for an equilibrium phase transition is based on the relaxation of the order parameter $m(t)$, which estimates the transition temperature, and a dynamical exponent. In the ferromagnetic (FM) case, it is expected that $m(t)$ decays to zero exponentially in the paramagnetic (PM) phase and to the value of the spontaneous magnetization m_{eq} in the FM phase. The algebraic decay appears at the critical temperature. The asymptotic behavior is summarized as

$$m(t) \sim \begin{cases} \exp(-t/\tau), & (T > T_c), \\ t^{-\lambda}, & (T = T_c), \\ m_{eq} & (T < T_c), \end{cases} \quad (3.1)$$

where τ is the relaxation time and λ is a dynamical exponent. Thus, if one plots $m(t)$ vs t on a double-logarithmic scale, one can recognize that the curves with upward trend indicate $T < T_c$ and those with downward trend indicate $T > T_c$ (as we will see in Figs. 2 and 4 below). To distinguish the phase from the asymptotic behavior of relaxation, the following logarithmic derivative of $m(t)$ is useful:

$$\lambda(t) = -\frac{d \ln m(t)}{d \ln t}. \quad (3.2)$$

The function $\lambda(t)$ is called a local exponent for the dynamical exponent λ. In practice, we estimate the transition temperature T_c from the temperature at which $\lambda(t)$ clearly approaches zero as the lower bound and that at which $\lambda(t)$ shows a diverging tendency as the upper bound. One determines the estimation of temperature as the center of these upper and lower bounds

and the error bar of it as their difference. It is noted that such a pinching estimation of T_c is reliable since the estimated error bar does not include a statistical uncertainty.

Another way to estimate the transition temperature from the numerically calculated NER of the order parameter, the dynamical scaling analysis has been applied frequently in the literature based on the following natural scaling form:

$$m(t, T) = \tau^{-\lambda} \Psi(t/\tau). \quad (3.3)$$

The relaxation time τ depends on the temperature and is expected to diverge at the transition temperature with the asymptotic form

$$\tau(T) = a|T - T_c|^{-b}. \quad (3.4)$$

Practically, we calculate $m(t, T)$ in a sufficient interval of Monte Carlo steps (MCSs) for several values of T. Let us use the label i for all data points as $m(t_i, T_i)$. The corresponding relaxation time is also dependent on i, i.e., τ_i, which should be identical for those with the same temperature, i.e., $\tau_i = \tau_j$ when $T_i = T_j$. If one assumes the scaling law, all data points converted as

$$X_i \equiv t_i/\tau_i, \quad (3.5)$$

$$Y_i \equiv \tau_i^{\lambda} m(t_i, T_i), \quad (3.6)$$

$$E_i \equiv \tau_i^{\lambda} \delta m(t_i, T_i) \quad (3.7)$$

should collapse according to the scaling function as

$$Y_i = \Psi(X_i), \quad (3.8)$$

where $\delta m(t_i, T_i)$ is the statistical error of $m(t_i, T_i)$ estimated in simulations and E_i is that of Y_i. Then, we fit the data to the above formula by adjusting parameters T_c, λ, a, and b.

Previously in the NER analysis, we used the pinching estimation to determine the transition temperature for second-order transitions instead of the dynamical scaling analysis because of the advantage of the lack of statistical uncertainty. Furthermore, in the scaling analysis, some problems arose; a model function for $\Psi(x)$ is necessary for the fitting procedure and so on. We have improved the analysis using the Bayesian statistics and the kernel method [29], which has two advantages over the old scaling approach. First, by means of the kernel method for constructing the scaling function, there is no ambiguity regarding the suitability of various scaling functions. This reduces the workload of a trial-and-error approach. Next, by means of the conjugate gradient method for minimizing the likelihood function, the scaling function can be optimized almost automatically and proceeds much faster. Note that this automation is another result of using the kernel method to guarantee a suitable trial function. These advantages enhance the usefulness of dynamical scaling analysis and provide the bootstrap method, which systematically gives precise estimates and their error bars.

In the present study, we adopt both the pinching method and the dynamical scaling for the chiral transition, which provides a reliable estimation for the transition temperature. For the determination of the upper and the lower bounds of the transition temperature, we avoid a plot of the local exponent $\lambda(t)$ vs $1/t$, which was used in previous NER analyses, since $\lambda(t)$ evaluated by numerical derivatives has shown ambiguous behaviors frequently in the vicinity of T_c. Instead of that,

we apply the improved dynamical scaling to confirm the determination of both bounds in the pinching procedure.

IV. CHIRAL TRANSITION TEMPERATURE

We analyze the chiral transition as a second-order one with the chiral order parameter Eq. (2.2), which is expected to decay as a power law

$$\kappa(t) \sim t^{-\lambda_\kappa} \qquad (4.1)$$

at $T = T_c$, where λ_κ is a dynamical exponent for the chiral transition.

A. Triangular-lattice system

In Fig. 2, we plot the relaxation of $\kappa(t)$ around the chiral-transition temperature for the triangular-lattice system. Hereafter we measure the temperature T in units of J/k_B. Let us consider an $L_x \times L_y$ lattice. For the purpose of efficient calculations, we use a skew boundary condition, where the boundary point (L_x, y) is connected to $(1, y+1)$ in the x direction, and (x, L_y) is connected to $(x-1, 1)$ and $(x, 1)$ in the y direction. To keep the consistency of the sublattice structure, this requires a lattice of $L \times (L+1)$, with $L = 3n - 1$. Calculations are carried out on a 4001×4002 lattice up to the observation time 10 000 MCSs. The linear size is twice as large as that in the previous paper with a five times longer observation. About 864 independent runs are performed for averaging. The size dependence is confirmed to be negligible when we compare the data with those on a 2000×2001 lattice for some temperatures.

For $0.5126 \leqslant T \leqslant 0.5145$, curves show a downward trend, indicating the disordered phase, and for $0.5096 \leqslant T \leqslant 0.5118$, curves show an upward trend, indicating the chiral phase. Thus, our estimation of the chiral-transition temperature in a pinching sense is $0.5118 < T_c < 0.5126$, providing $T_c = 0.5122(4)$. Note that we remove some temperatures close to T_c in which the phase cannot be distinguished from the trend of the relaxation. This observation was confirmed by the plot of $\lambda_\kappa(t)$ vs $1/t$ previously, while we will achieve it by using the improved dynamical scaling as follows.

We apply the dynamical scaling analysis to estimate and confirm a precise transition temperature. We use data for 10–12 temperatures for both regions of $T > T_c$ and $T < T_c$, as shown in Fig. 2. The scaling procedure for Eq. (3.3) is performed for the data for $T > T_c$ and for $T < T_c$ separately. The results are shown together in Fig. 3 with the estimation $T_c = 0.5123$ for the data in the high-temperature regime and $T_c = 0.5119$ in the low-temperature regime. These estimations of T_c obtained by the dynamical scaling are consistent with that obtained with the pinching one, $T_c = 0.5122(4)$, which indicates the validity of the separation of two regimes in Fig. 2 and the accuracy and reliability of the estimation. This result has an order of magnitude better accuracy than the previous paper [27].

B. Square-lattice system

In Fig. 4, we plot the relaxation of $\kappa(t)$ around the chiral-transition temperature for the square-lattice system. Unlike for the triangular-lattice system, we use a double-skew boundary
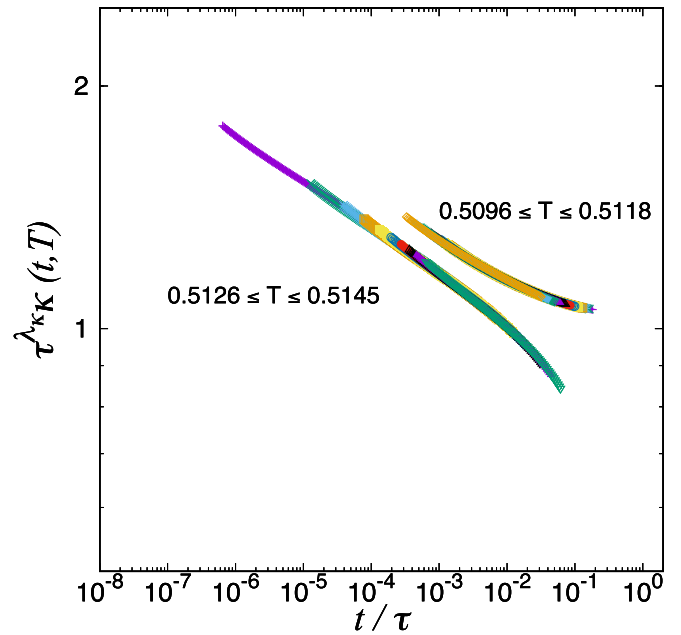

FIG. 3. Scaling plots of $\kappa(t, T)$ in Fig. 2 for the triangular-lattice system. The scaling function is shown separately for temperatures with an upward trend, $0.5096 \leqslant T \leqslant 0.5118$, and those with a downward trend, $0.5126 \leqslant T \leqslant 0.5145$, in which the transition temperature is estimated as $T_c = 0.5119$ and $T_c = 0.5123$, respectively.

condition for the square-lattice system. In this condition, the boundary point (L_x, y) is connected to $(1, y+2)$ in the x direction, and (x, L_y) is connected to $(x, 1)$ in the y direction. This requires a lattice of $L \times L$ with $L = 2n$. Calculations are carried out on a 4000×4000 lattice up to the observation time 10 000 MCSs. The linear size is twice as large as that
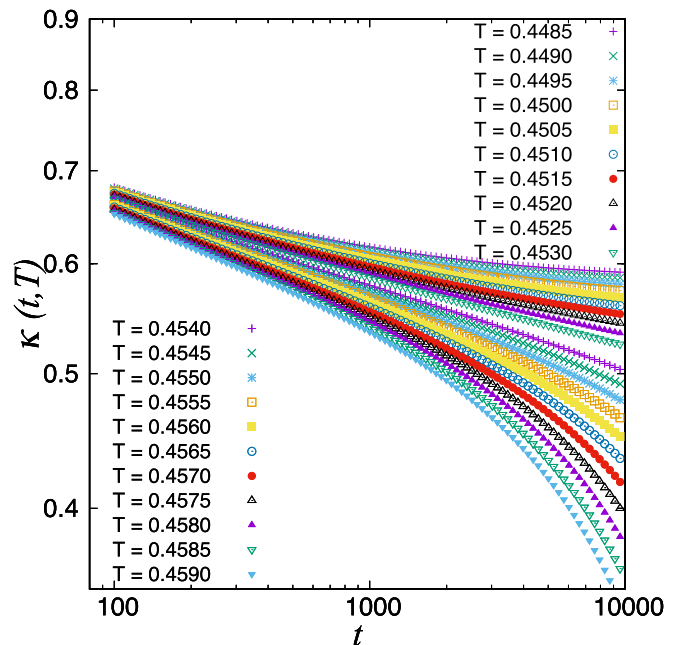

FIG. 4. Relaxation of the chiral order parameter $\kappa(t, T)$ for the square-lattice system in $0.4485 \leqslant T \leqslant 0.4530$ and in $0.4540 \leqslant T \leqslant 0.4590$ plotted on a double-logarithmic scale.
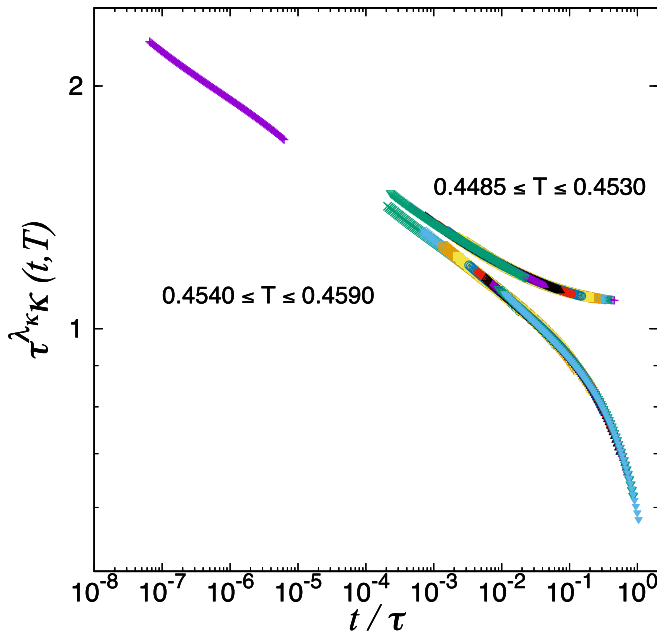
FIG. 5. Scaling plot of $\kappa(t, T)$ in Fig. 4 for the square-lattice system. The scaling function is shown separately for temperatures with an upward trend, $0.4485 \leqslant T \leqslant 0.4530$, and those with a downward trend, $0.4540 \leqslant T \leqslant 0.4590$, in which the transition temperature is estimated as $T_c = 0.4529$ and $T_c = 0.4531$, respectively.

in the previous paper with a five times longer observation. About 864 independent runs are performed for averaging. The size dependence is confirmed to be negligible when we compare the data with those on a 2000×2000 lattice for some temperatures.

For $0.4540 \leqslant T \leqslant 0.4590$, curves show a downward trend, indicating the disordered phase, and for $0.4485 \leqslant T \leqslant 0.4530$, curves show an upward trend, indicating the chiral phase. Thus, our estimation of the chiral-transition temperature in the pinching sense is $0.4530 < T_c < 0.4540$, providing $T_c = 0.4535(5)$. As in the triangular-lattice case, we remove some temperatures close to T_c in which the behaviors of the relaxation cannot identify the phase. We will confirm this estimation by using the improved dynamical scaling as follows.

We prepare relaxation data for 10^4 MCS points for each temperature. We use data for 10 to 11 temperatures, as shown in Fig. 4. The scaling procedure for Eq. (3.3) is performed for the data for $T > T_c$ and for $T < T_c$ separately. The results are shown together in Fig. 5 with the estimation $T_c = 0.4531$ for the data in the high-temperature regime and $T_c = 0.4529$ in the low-temperature regime. These estimations of T_c obtained with the dynamical scaling are almost consistent with that obtained with the pinching one, $T_c = 0.4535(5)$, which indicates the validity of the separation of two regimes in Fig. 4 and the accuracy and reliability of the estimation.

V. UNIVERSALITY CLASS OF THE CHIRAL TRANSITION

We investigate the validity of the conclusion on the universality class of the chiral transition discussed in the previous paper [27]. Our aim is to calculate the asymptotic behavior

of local exponents by calculating the NER of fluctuations for longer MCSs, in which lager lattices would be necessary to avoid the appearance of size dependency. Thus, we perform simulations for longer MCSs on larger lattices than those in the previous paper at the chiral critical temperature updated in Sec. IV.

Let us explain the method for evaluation. The local exponent of $\kappa(t)$ is defined by a logarithmic derivative,

$$\lambda_\kappa(t) = -\frac{d \ln \kappa(t)}{d \ln t}. \tag{5.1}$$

It is confirmed that the relaxation of dimensionless fluctuations,

$$f_{\kappa\kappa}(t) \equiv N \left[\frac{\langle \kappa(t)^2 \rangle}{\langle \kappa(t) \rangle^2} - 1 \right] \tag{5.2}$$

and

$$f_{\kappa e}(t) \equiv N \left[\frac{\langle \kappa(t)e(t) \rangle}{\langle \kappa(t) \rangle \langle e(t) \rangle} - 1 \right], \tag{5.3}$$

show power-law divergences

$$f_{\kappa\kappa}(t) \sim t^{\lambda_{\kappa\kappa}} \tag{5.4}$$

and

$$f_{\kappa e}(t) \sim t^{\lambda_{\kappa e}} \tag{5.5}$$

at the critical point, where $e(t)$ is the energy per site [26,31]. Assuming the dynamical scaling hypothesis, one derives relations for the asymptotic powers of relaxation functions with the standard critical exponents as

$$\lambda_\kappa = \beta/z\nu, \quad \lambda_{\kappa\kappa} = d/z, \quad \lambda_{\kappa e} = 1/z\nu. \tag{5.6}$$

The local exponents $\lambda_{\kappa\kappa}(t)$ and $\lambda_{\kappa e}(t)$ are also defined by similar logarithmic derivatives as in Eq. (5.1). Thus, one can estimate each exponent asymptotically from a combination of the local exponents, i.e.,

$$z(t) = \frac{d}{\lambda_{\kappa\kappa}(t)}, \quad \nu(t) = \frac{\lambda_{\kappa\kappa}(t)}{d\lambda_{\kappa e}(t)}, \quad \eta(t) = \frac{2d\lambda_\kappa(t)}{\lambda_{\kappa\kappa}(t)}. \tag{5.7}$$

In Fig. 6, we plot $f_{\kappa\kappa}(t)$ and $f_{\kappa e}(t)$ on a double-logarithmic scale for the triangular-lattice system at $T_c = 0.5122$ on a 1001×1002 lattice. Calculations are carried out up to the observation time of 2000 MCS with 1 555 200 independent runs for averaging; the linear size is twice as large as that in the previous paper with a four times longer observation. For the square-lattice system, similar calculations are made up to the observation time of 2000 MCSs with 1 036 800 independent runs at $T_c = 0.4535$ on a 1500×1500 lattice, and $f_{\kappa\kappa}(t)$ and $f_{\kappa e}(t)$ are plotted in Fig. 7; the linear size is three times as large as that in the previous paper with a four times longer observation. For both lattice systems, asymptotic divergences are observed as mentioned above.

Next, we evaluate the local exponents $\lambda_\kappa(t)$, $\lambda_{\kappa\kappa}(t)$, and $\lambda_{\kappa e}(t)$ defined in Eqs. (5.1), (5.4), and (5.5) by means of numerical derivative and calculate the local exponents for the conventional critical exponents, $z(t)$, $\eta(t)$, and $\nu(t)$, defined in Eq. (5.7). The results for both lattice systems are shown together by solid symbols in Figs. 8, 9, and 10. The results in the previous study [27] are also plotted by open symbols, where shorter MCSs and smaller lattices were used. In these
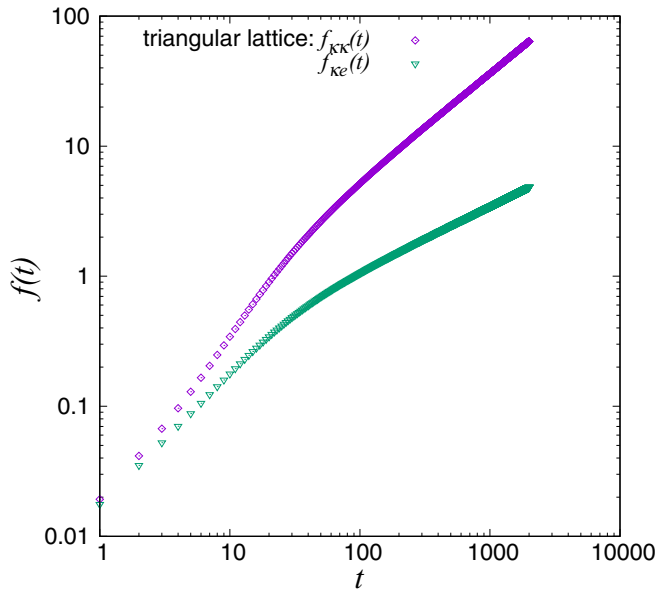
FIG. 6. Relaxation functions of fluctuations, $f_{\kappa\kappa}(t)$ and $f_{\kappa e}(t)$, at the estimated chiral transition temperature ($T_c = 0.5122$) for the triangular-lattice system. They are plotted on a double-logarithmic scale.

FIG. 8. Local exponent $z(t)$ for the triangular-lattice system (triangles) and for the square-lattice system (squares). Solid symbols represent present results. Open symbols represent previous results reported in Ref. [27]. The solid and dashed lines are the best fit to the data in asymptotic regime.

figures, estimated exponents are plotted versus $1/t^\Omega$. We set $\Omega = 1$ for $z(t)$ and $\eta(t)$ and $\Omega = 0.793$ for $\nu(t)$, following the previous study, in which, for each plot, it was chosen so that the linearity of the curves is good in the asymptotic regime (around $1/t \sim 0$) to estimate the exponent precisely. In each figure, the best fits for the present data (solid symbols) in the asymptotic regime are represented by dotted lines. These fits provide the values of the estimation and the error bars. For the triangular-lattice system, we estimate $z = 2.43(2)$, $\eta =$
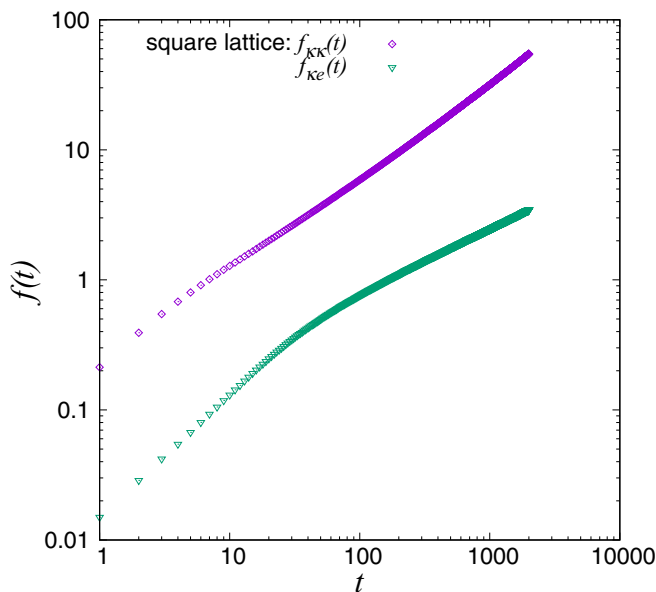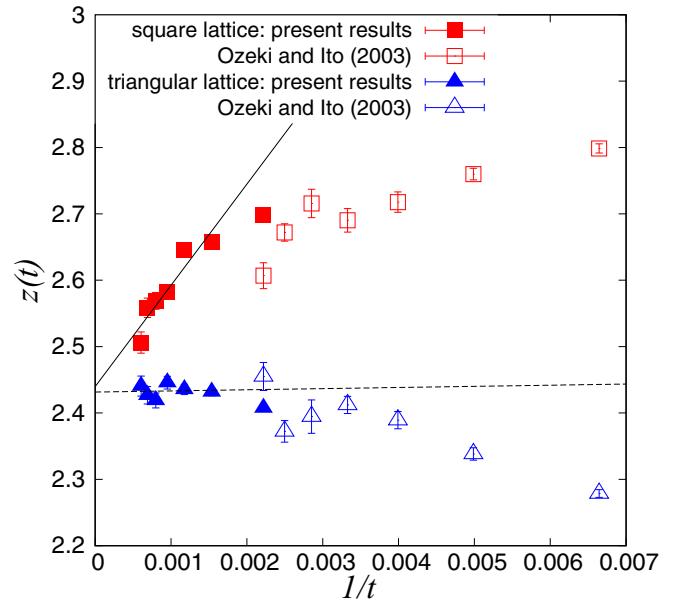
$0.229(2)$, and $\nu = 0.817(14)$. For the square-lattice system, we estimate $z = 2.44(4)$, $\eta = 0.233(4)$, and $\nu = 0.824(9)$. The results are summarized in Table I. The estimated exponents show almost identical values, indicating a unified critical universality class.

We can see the consistency of plots between the present study and the previous ones in several ways. First, the linearity of the curves for the present data seems to be almost

FIG. 7. Relaxation functions of fluctuations, $f_{\kappa\kappa}(t)$ and $f_{\kappa e}(t)$, at the estimated chiral transition temperature ($T_c = 0.4535$) for the square-lattice system.
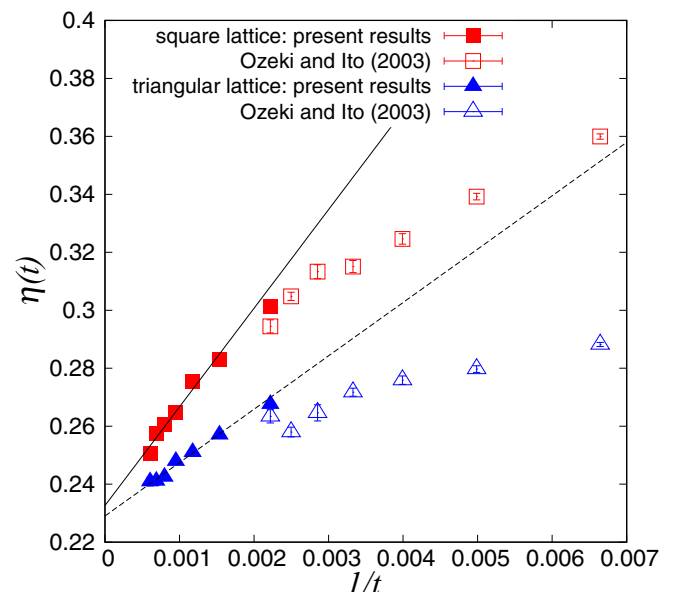

FIG. 9. Local exponent $\eta(t)$. The symbols are the same as those in Fig. 8.

FIG. 10. Local exponent $\nu(t)$. The symbols are the same as those in Fig. 8.

TABLE I. Summary of resulting transition temperatures and critical exponents for both lattice systems.

Lattice	T_c	z	η	ν	T_{KT}
Triangular	0.5122(4)	2.43(2)	0.229(2)	0.817(14)	0.5085(2)
Square	0.4535(5)	2.44(4)	0.233(4)	0.824(9)	0.4493(2)

as mentioned above; we conclude that this criticism is inappropriate.

VI. KT TRANSITION TEMPERATURE

The improved dynamical scaling also provides a reliable estimation for KT transition temperatures. We have applied it to the present models to clarify the double transitions concluded previously. Here, we estimate them for both lattice systems with longer MCSs and lager lattices by the use of improved dynamical scaling analysis [29,30] to confirm and support the picture of the double transitions.

The NER analysis of the order parameter can be applied to the case of the KT transition, although some difficulties arise. The asymptotic behavior of the order parameter $m_O(t)$ defined in (2.3) is expected to be

$$m_O(t) \sim \begin{cases} \exp(-t/\tau), & (T > T_{KT}), \\ t^{-\lambda(T)}, & (T \leqslant T_{KT}). \end{cases} \quad (6.1)$$

The dynamical exponent $\lambda(T)$, the asymptotic power of the relaxation, is defined entirely in the KT phase and depends on the temperature. Only the upper bound of T_{KT} is estimated, while the lower bound cannot be. Thus, one cannot use the pinching method or estimate a reliable error bar as discussed in Sec. III. To confirm the KT transition and estimate the transition temperature, we have introduced the dynamical scaling analysis based on Eq. (3.3) with the asymptotics of the relaxation time [26,32]

$$\tau(T) = a \exp\left(\frac{b}{\sqrt{T - T_{KT}}}\right), \quad (6.2)$$

instead of Eq. (3.4) for second-order transition cases.

For the triangular-lattice system, calculations are carried out on the 2000×2001 lattice up to the observation time of 5×10^5 MCSs. The linear size is twice as large as that in the previous paper with a five times longer observation. About 864 independent runs are performed for averaging. The size dependence is confirmed to be negligible. The result is plotted in Fig. 11. To estimate T_{KT} precisely, we apply the improved dynamical scaling analysis explained in Sec. III. The scaling plot is shown in Fig. 12. We estimate the error bar using the bootstrap method with 100 samples and get the transition temperature as $T_{KT} = 0.5085(2)$. This result has an order of magnitude better accuracy than that in the previous paper [27]. Thus, the chiral transition temperature estimated as $T_c = 0.5122(2)$ is clearly separated with T_{KT} indicating the double transition.

For the square-lattice system, a similar analysis is made on the 2000×2000 lattice up to the observation time of 5×10^5 MCSs. The linear size is twice as large as that in the previous paper with a five times longer observation. About
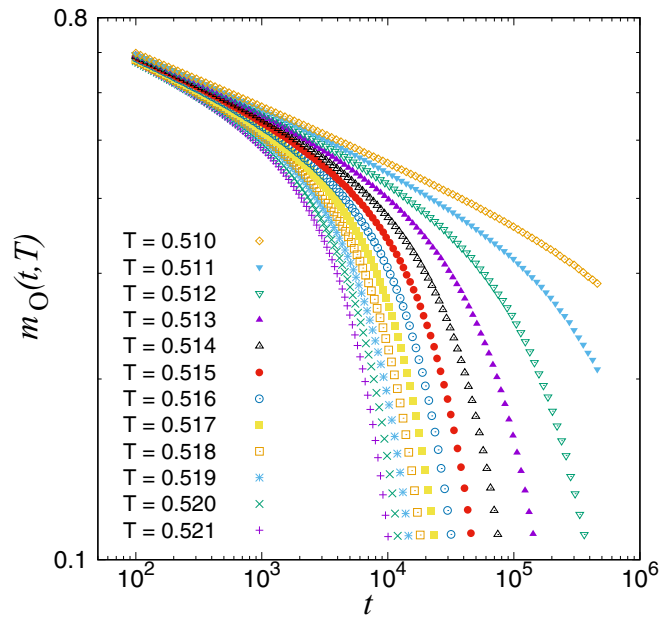
good, even if the old Ω's are used. Second, the continuity of asymptotic behaviors in the previous data seems consistent with those in the present ones in which they are estimated with longer MCSs and larger lattices.[1] The extrapolated critical exponents in the previous study indicated almost the same values between the triangular-lattice system and the square-lattice one. It was mentioned that this indicated the unified universality class for the FFXY models in two dimensions. In the present results, the asymptotic behaviors in Figs. 8–10 support this picture more clearly and precisely because of the longer observation. As in the previous paper, the closeness of the estimated exponents obtained independently for the present two models supports the validity of the picture of the non-Ising class. As seen especially in Fig. 10, the asymptotic behavior of $\nu(t)$ for the triangular-lattice system appears (slightly) decreasing for $1/t \to 0$ and would not indicate the tendency to approach the Ising value ($\nu = 1$), even if a relaxation in longer MCSs was observed.

There has been criticism [22,28] that similar results indicating a non-Ising class obtained with EMCS with finite-size scaling analysis are an artifact due to the smallness of the simulated lattices. Obuchi and Kawamura [28] further claimed that the previous NER result [27] was also an artifact due to the shortness of simulated observations. While much larger lattices are simulated in the present study, we need to pay attention to the finite-time effect instead of the finite-size one in the NER analysis. As seen in Figs. 8–10, the asymptotic behaviors are expected to converge to the estimated values. The reliability has been improved in the present estimations

---

[1]In Figs. 8–10, we remove the shortest time point of the present estimation, i.e., $1/t = 0.04$, since it includes the initial relaxation, which deviates from the asymptotic behavior.

FIG. 11. Relaxation of the spin orientational order parameter $m_O(t, T)$ in $0.510 \leqslant T \leqslant 0.521$ for the triangular-lattice system plotted on a double-logarithmic scale.
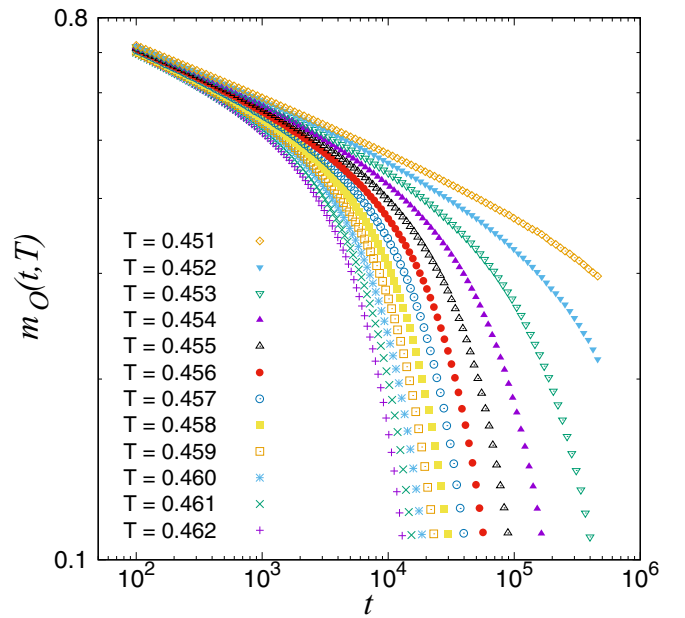

FIG. 13. Relaxation of the spin order parameter $m_O(t, T)$ in $0.451 \leqslant T \leqslant 0.462$ for the square-lattice system plotted on a double-logarithmic scale.

864 independent runs are performed for averaging. The result is plotted in Fig. 13. To estimate T_{KT} precisely, we used the improved dynamical scaling analysis. The scaling plot is shown in Fig. 14. We calculate the transition temperature using the bootstrap method, as $T_{KT} = 0.4493(2)$. This result has an order of magnitude better accuracy than the previous paper [27]. Thus, the chiral transition temperature estimated as $T_c = 0.4535(5)$ is clearly separated with T_{KT} indicating the double transition.

For both models, we have clearly observed the difference of T_c and T_{KT}, which indicates the double transition and the existence of the intermediate phase [3,4]. It is noted that the transition temperature T_{KT} is estimated by the scaling analysis. While we believe our numerical estimations are accurate, it would be valuable to see the double-transition phenomenon definitely. For the triangular-lattice system, the chiral transition clearly occurs at $0.5118 < T_c < 0.5126$ (see Fig. 2), which is regarded as a result of the thermodynamic limit. On
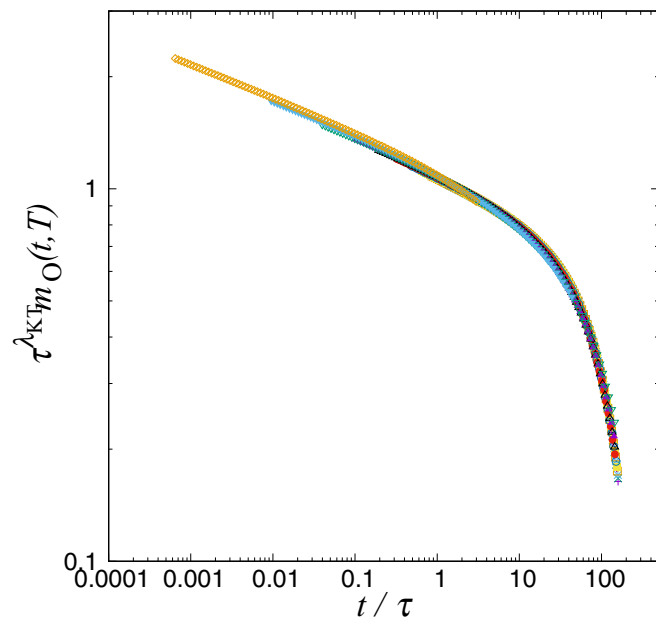

FIG. 12. Scaling plot of $m_O(t, T)$ in Fig. 11, where the transition temperature is estimated as $T_c = 0.5085$.
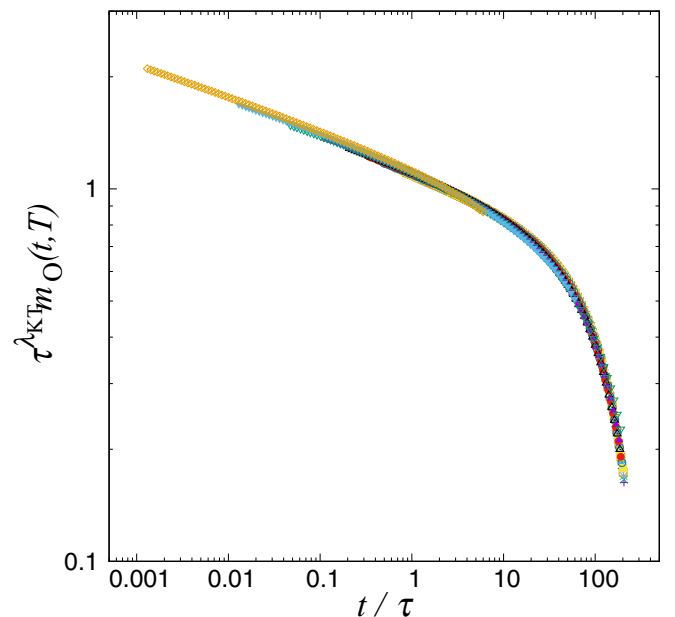

FIG. 14. Scaling plot of $m_O(t, T)$ in Fig. 13, where the transition temperature is estimated as $T_c = 0.4493$.

the other hand, the KT transition must occur at $T_{\mathrm{KT}} < 0.510$, which is confirmed by the asymptotic downward trend at $T = 0.510$ in Fig. 11. Therefore, at least at $0.510 < T < 0.5118$, which is a modest estimation, an intermediate phase appears. The same argument can be made for the result of the square-lattice system; at least at $0.451 < T < 0.4530$ (see Figs. 4 and 13), an intermediate phase appears. Consequently, we have numerically confirmed the double transition in the FFXY models in two dimensions.

VII. SUMMARY

We have investigated the critical properties of fully frustrated XY models on triangular and square lattices by means of the nonequilibrium relaxation method. The dynamical scaling analysis was applied, which was recently improved by the kernel method [29,30]. The chiral transition temperature and the Kosterlitz-Thouless one were estimated precisely. Using the NER of fluctuations, the critical exponents of the chiral transition were also estimated. The numerical results are summarized in Table I. The validity of the previous conclusion was examined for the universality class of the chiral transition, in which that belongs to a non-Ising-type one. We analyzed the NER of fluctuations for longer Monte

Carlo steps on lager lattices than those performed previously. The calculation was made at chiral transition temperatures updated precisely. The result indicates that the asymptotic behavior of the time-dependent exponents, which should converge to the critical exponents, shows the same tendency as those obtained for shorter MCSs. We also applied the improved dynamical scaling analysis to the estimation of KT transitions, and the existence of the double transitions for the chiral and KT phases was confirmed with more reliable estimations.

The simulated size is large enough to eliminate the finite-size effect; however, the finite-time observation cannot avoid the possibility of crossover phenomena which could modify the physics. While we showed that such a possibility would not be the case in the present study, further investigations with longer-MCS observations would be helpful to confirm the conclusions definitely.

ACKNOWLEDGMENTS

[1] J. Villain, J. Phys. C **10**, 4793 (1977).

[2] J. Villain, J. Phys. (Paris) **38**, 26 (1977).

[3] S. Teitel and C. Jayaprakash, Phys. Rev. B **27**, 598(R) (1983).

[4] S. Miyashita and H. Shiba, J. Phys. Soc. Jpn. **53**, 1145 (1984).

[5] D. H. Lee, J. D. Joannopoulos, J. W. Negele, and D. P. Landau, Phys. Rev. Lett. **52**, 433 (1984).

[6] M. Y. Choi and S. Doniach, Phys. Rev. B **31**, 4516 (1985).

[7] M. Yosefin and E. Domany, Phys. Rev. B **32**, 1778 (1985).

[8] M. Y. Choi and D. Stroud, Phys. Rev. B **32**, 5773 (1985).

[9] J. E. Van Himbergen, Phys. Rev. B **33**, 7857 (1986).

[10] J. Lee, J. M. Kosterlitz, and E. Granato, Phys. Rev. B **43**, 11531 (1991).

[11] S. Lee and K. C. Lee, Phys. Rev. B **57**, 8472 (1998).

[12] S. E. Korshunov, Phys. Rev. Lett. **88**, 167007 (2002).

[13] B. Berge, H. T. Diep, A. Ghazali, and P. Lallemand, Phys. Rev. B **34**, 3177 (1986).

[14] G. S. Grest, Phys. Rev. B **39**, 9267 (1989).

[15] J. M. Thijssen and H. J. F. Knops, Phys. Rev. B **42**, 2438 (1990).

[16] E. Granato and M. P. Nightingale, Phys. Rev. B **48**, 7438 (1993).

[17] J. R. Lee, Phys. Rev. B **49**, 3317 (1994).

[18] G. Ramirez-Santiago and J. V. José, Phys. Rev. B **49**, 9567 (1994).

[19] S. Lee and K. C. Lee, Phys. Rev. B **49**, 15184 (1994).

[20] Y. M. M. Knops, B. Nienhuis, H. J. F. Knops, and H. W. J. Blöte, Phys. Rev. B **50**, 1061 (1994).

[21] P. Olsson, Phys. Rev. Lett. **75**, 2758 (1995).

[22] P. Olsson, Phys. Rev. B **55**, 3585 (1997).

[23] G. S. Jeon, S. Y. Park, and M. Y. Choi, Phys. Rev. B **55**, 14088 (1997).

[24] H. J. Luo, L. Schülke, and B. Zheng, Phys. Rev. Lett. **81**, 180 (1998).

[25] H. J. Luo, L. Schülke, and B. Zheng, Phys. Rev. E **57**, 1327 (1998).

[26] Y. Ozeki and N. Ito, J. Phys. A **40**, R149 (2007).

[27] Y. Ozeki and N. Ito, Phys. Rev. B **68**, 054414 (2003).

[28] T. Obuchi and H. Kawamura, J. Phys. Soc. Jpn. **81**, 054003 (2012).

[29] Y. Echinaka and Y. Ozeki, Phys. Rev. E **94**, 043312 (2016).

[30] Y. Ozeki, A. Matsuda, and Y. Echinaka, Phys. Rev. E **99**, 012116 (2019).

[31] Y. Ozeki, N. Ito, and K. Ogawa, J. Phys. Soc. Jpn. **70**, 3471 (2001).

[32] Y. Ozeki, K. Ogawa, and N. Ito, Phys. Rev. E **67**, 026702 (2003).